© ESO 2004



First detection of triply-deuterated methanol

B. Parise¹, A. Castets², E. Herbst³, E. Caux¹, C. Ceccarelli⁴, I. Mukhopadhyay⁵, and A. G. G. M. Tielens⁶

- ¹ CESR CNRS-UPS, BP 4346, 31028 Toulouse Cedex 04, France
- ² Observatoire de Bordeaux, BP 89, 33270 Floirac, France
- ³ Department of Physics, The Ohio State University, 174 W. 18th Ave. Columbus, OH 43210-1106, USA
- ⁴ Laboratoire d'Astrophysique, Observatoire de Grenoble, BP 53, 38041 Grenoble Cedex 09, France
- ⁵ Dakota State University, 820 N. Washington Ave., Madison, SD 57042, USA
- ⁶ SRON, PO Box 800, 9700 AV Groningen, The Netherlands

Received 7 August 2003 / Accepted 3 November 2003

Abstract. We report the first detection of triply-deuterated methanol, with 12 observed transitions, towards the low-mass protostar IRAS 16293–2422, as well as multifrequency observations of 13 CH₃OH, used to derive the column density of the main isotopomer CH₃OH. The derived fractionation ratio [CD₃OH]/[CH₃OH] averaged on a 10" beam is 1.4%. Together with previous CH₂DOH and CHD₂OH observations, the present CD₃OH observations are consistent with a formation of methanol on grain surfaces, if the atomic D/H ratio is 0.1 to 0.3 in the accreting gas. Such a high atomic ratio can be reached in the framework of gas-phase chemical models including all deuterated isotopomers of H_3^+ .

Key words. ISM: abundances – ISM: molecules – stars: formation – ISM: individual: IRAS 16293–2422

1. Introduction

Despite the relatively low elemental abundance of deuterium in space (a factor of $\sim 1.5 \times 10^{-5}$ less abundant than H; Linsky 1998), extremely large amounts of doubly-deuterated formaldehyde ($D_2CO/H_2CO \sim 10\%$) have been observed in the solar-type protostar IRAS 16293-2422 (hereafter IRAS 16293, Ceccarelli et al. 1998; Loinard et al. 2000; Ceccarelli et al. 2001), initiating the search for other multiply deuterated molecules. Subsequently, doubly deuterated formaldehyde, doubly deuterated hydrogen sulfide and multiply deuterated ammonia have been observed in other protostars and dark clouds from where protostars form (Roueff et al. 2000; Loinard et al. 2001; Ceccarelli et al. 2002; van der Tak et al. 2002; Lis et al. 2002; Vastel et al. 2003). These studies have been interpreted in terms of two different routes for formaldehyde, hydrogen sulfide and ammonia deuteration: active grain chemistry followed by at least partial desorption into the gas for formaldehyde and hydrogen sulfide on the one hand and gas-phase chemistry for ammonia on the other hand. However, ammonia may also be a grain surface product, provided a large D/H atomic ratio in the accreting gas. Recently, doubly-deuterated methanol was detected towards IRAS 16293 (Parise et al. 2002). This observation provided new constraints for chemical models. The observations of the deuterated methanols CH2DOH and CHD2OH were both consistent with the formation of methanol from successive hydrogenations of CO by reaction with atomic H on

Send offprint requests to: B. Parise, e-mail: Berengere.Parise@cesr.fr

grain surfaces, but required an atomic D/H ratio of 0.2 to 0.3 in the accreting gas. At the time of the observation of doublydeuterated methanol, no gas-phase model was able to predict such a high atomic D/H ratio. Meantime, observations of doubly deuterated formaldehyde in a sample of pre-stellar cores showed that the degree of deuteration increases with increasing CO depletion (Bacmann et al. 2002, 2003). This deuteration of formaldehyde in pre-stellar cores may occur partially in the CO-depleted gas-phase and partially on the surface of dust grains, followed by some inefficient desorption mechanism. A further spectacular confirmation of enhanced deuteration in CO-depleted gas came from the detection of abundant H₂D⁺, likely the most abundant ion, in the prestellar core L1544 (Caselli et al. 2003). Phillips & Vastel (2003) suggested that in CO-depleted gas, even the multiple deuterated forms of H₃ may be abundant and play a role in the molecular deuteration enhancement. The suggestion has been fully confirmed by the modelling of Roberts et al. (2003), which shows that including HD₂ and D₃ in the chemical network increases dramatically the molecular deuteration, and allows the production of the large atomic D/H ratio predicted by the methanol observations (Parise et al. 2002).

In this paper, we report the first detection of triply-deuterated methanol CD₃OH in space, performed towards the solar-type protostar IRAS 16293. We also present a multifrequency observation of ¹³CH₃OH, used to derive the column density of the main isotopomer CH₃OH. These observations provide yet another stringent test to confirm the validity of grain surface models.

Table 1. Main-beam intensities¹, peak temperatures² and widths for the observed CD₃OH and ¹³CH₃OH transitions³.

$ \begin{array}{c ccccccccccccccccccccccccccccccccccc$			2		C — .		
$\begin{array}{c} \text{CD}_3\text{OH} \\ \hline 156.237016^* & 4_{1}-3_{1} \text{ E}_{2} & 2.94 & 21.5 & 0.102 \pm 0.023 & 51 & 1.8 \pm 0.4 \\ 156.239295 & 4_{2}-3_{2} \text{ A}- & 2.44 & 42.0 & 0.032 \pm 0.012 & 26 & 1.2 \pm 0.5 \\ 156.242613 & 4_{0}-3_{0} \text{ A}+ & 3.13 & 18.8 & 0.059 \pm 0.018 & 31 & 1.8 \pm 0.5 \\ 156.253079 & 4_{2}-3_{2} \text{ A}+ & 2.44 & 42.0 & 0.056 \pm 0.015 & 38 & 1.4 \pm 0.4 \\ 156.260737^* & 4_{3}-3_{3} \text{ E}_{2} & 1.39 & 55.5 & 0.061 \pm 0.018 & 46 & 1.3 \pm 0.4 \\ 156.262936 & 4_{3}-3_{3} \text{ E}_{1} & 1.37 & 46.9 & 0.044 \pm 0.011 & 43 & 1.0 \pm 0.2 \\ 156.275238 & 4_{1}-3_{1} \text{ E}_{1} & 2.93 & 33.1 & 0.034 \pm 0.021 & 26 & 1.2 \pm 1.2 \\ 156.285288^* & 4_{2}-3_{2} \text{ E}_{2} & 2.35 & 36.3 & 0.065 \pm 0.021 & 54 & 1.1 \pm 0.3 \\ 156.581519 & 8_{1}-7_{0} \text{ E}_{2} & 4.15 & 70.2 & 0.050 \pm 0.010 & 46 & 1.0 \pm 0.2 \\ 160.640122 & 2_{0}-2_{1} \text{ E}_{2} & 2.38 & 15.95 & 0.090 \pm 0.019 & 26 & 3.2 \pm 0.5 \\ 160.718291 & 6_{2}-5_{1} \text{ E}_{1} & 2.22 & 50.2 & 0.039 \pm 0.009 & 29 & 1.3 \pm 0.2 \\ 160.53934 & 1_{0}-1_{1} \text{ E}_{2} & 1.45 & 12.2 & 0.038 \pm 0.009 & 35 & 1.0 \pm 0.2 \\ \hline 1^{3}\text{CH}_{3}\text{OH} & & & & & & & & & & & & & & & & & \\ \hline 156.299374 & 5_{05}-5_{-15} & 0.697 & 47.1 & 0.19 \pm 0.08 & 65 & 3.0 \pm 0.5 \\ 160.507694 & 2_{12}-3_{03} & 0.300 & 21.3 & 0.08 \pm 0.02 & 29 & 2.4 \pm 0.6 \\ 330.194042 & 7_{-17}-6_{-16} & 5.55 & 69.0 & 0.51 \pm 0.16 & 120 & 3.8 \pm 0.6 \\ 330.252798 & 7_{07}-6_{06} & 5.66 & 63.4 & 0.43 \pm 0.15 & 100 & 4.0 \pm 1.2 \\ 330.265233 & 7_{-61}-6_{-60} & 1.50 & 253.4 & 0.15 \pm 0.10 & 80 & 1.7 \pm 1.0 \\ 330.277270 & 7_{62}-6_{61} & 1.50 & 258.1 & 0.12 \pm 0.08 & 60 & 2.0 \pm 0.7 \\ 330.319110 & 7_{52}-6_{51} & 2.78 & 202.0 & 0.45 \pm 0.21 & 90 & 4.8 \pm 0.9 \\ 330.319110 & 7_{53}-6_{52} & 2.78 & 202.0 & 0.45 \pm 0.21 & 90 & 4.8 \pm 0.9 \\ 330.342534 & 7_{44}-6_{43} & 3.81 & 144.2 & 0.07 \pm 0.05 & 50 & 1.3 \pm 6.7 \\ 330.442421 & 7_{16}-6_{15} & 5.69 & 84.49 & 0.42 \pm 0.12 & 140 & 2.8 \pm 0.9 \\ 330.535822 & 7_{25}-6_{24} & 5.14 & 85.80 & 0.25 \pm 0.11 & 40 & 5.6 \pm 1.2 \\ \hline \end{tabular}$	Frequency	Transition	$\mu^2 S$	$E_{ m up}$	$\int T_{ m mb} { m d}v$	$T_{ m mb}$	Δv
$\begin{array}{cccccccccccccccccccccccccccccccccccc$			Debye ²	K	K km s ⁻¹	mK	km s ⁻¹
$\begin{array}{cccccccccccccccccccccccccccccccccccc$							
$\begin{array}{cccccccccccccccccccccccccccccccccccc$	156.237016*	$4_1 - 3_1 E_2$	2.94	21.5	0.102 ± 0.023	51	1.8 ± 0.4
$\begin{array}{cccccccccccccccccccccccccccccccccccc$	156.239295	$4_2 - 3_2 A -$	2.44	42.0	0.032 ± 0.012	26	1.2 ± 0.5
$\begin{array}{c} 156.260737^* & 4_3-3_3 \ E_2 & 1.39 & 55.5 & 0.061 \pm 0.018 & 46 & 1.3 \pm 0.4 \\ 156.262936 & 4_3-3_3 \ E_1 & 1.37 & 46.9 & 0.044 \pm 0.011 & 43 & 1.0 \pm 0.2 \\ 156.275238 & 4_1-3_1 \ E_1 & 2.93 & 33.1 & 0.034 \pm 0.021 & 26 & 1.2 \pm 1.2 \\ 156.285288^* & 4_2-3_2 \ E_2 & 2.35 & 36.3 & 0.065 \pm 0.021 & 54 & 1.1 \pm 0.3 \\ 156.581519 & 8_1-7_0 \ E_2 & 4.15 & 70.2 & 0.050 \pm 0.010 & 46 & 1.0 \pm 0.2 \\ 160.640122 & 2_0-2_1 \ E_2 & 2.38 & 15.95 & 0.090 \pm 0.019 & 26 & 3.2 \pm 0.5 \\ 160.718291 & 6_2-5_1 \ E_1 & 2.22 & 50.2 & 0.039 \pm 0.009 & 29 & 1.3 \pm 0.2 \\ 160.753934 & 1_0-1_1 \ E_2 & 1.45 & 12.2 & 0.038 \pm 0.009 & 35 & 1.0 \pm 0.2 \\ \hline \\ 13^3 \ CH_3 \ OH & & & & & & & & & & & & & & & & & & $	156.242613	$4_0 - 3_0 \text{ A} +$	3.13	18.8	0.059 ± 0.018	31	1.8 ± 0.5
$\begin{array}{cccccccccccccccccccccccccccccccccccc$	156.253079	$4_2 - 3_2 A +$	2.44	42.0	0.056 ± 0.015	38	1.4 ± 0.4
$\begin{array}{cccccccccccccccccccccccccccccccccccc$	156.260737*	$4_3 - 3_3 E_2$	1.39	55.5	0.061 ± 0.018	46	1.3 ± 0.4
$\begin{array}{c ccccccccccccccccccccccccccccccccccc$	156.262936	$4_3 - 3_3 E_1$	1.37	46.9	0.044 ± 0.011	43	1.0 ± 0.2
$\begin{array}{cccccccccccccccccccccccccccccccccccc$	156.275238	$4_1 - 3_1 E_1$	2.93	33.1	0.034 ± 0.021	26	1.2 ± 1.2
$\begin{array}{cccccccccccccccccccccccccccccccccccc$	156.285288*	$4_2 - 3_2 E_2$	2.35	36.3	0.065 ± 0.021	54	1.1 ± 0.3
$\begin{array}{c ccccccccccccccccccccccccccccccccccc$	156.581519	$8_1 - 7_0 E_2$	4.15	70.2	0.050 ± 0.010	46	1.0 ± 0.2
$\begin{array}{c ccccccccccccccccccccccccccccccccccc$	160.640122	$2_0-2_1 E_2$	2.38	15.95	0.090 ± 0.019	26	3.2 ± 0.5
$\begin{array}{c ccccccccccccccccccccccccccccccccccc$	160.718291	$6_2 - 5_1 E_1$	2.22	50.2	0.039 ± 0.009	29	1.3 ± 0.2
$\begin{array}{cccccccccccccccccccccccccccccccccccc$	160.753934	$1_0 - 1_1 E_2$	1.45	12.2	0.038 ± 0.009	35	1.0 ± 0.2
$\begin{array}{cccccccccccccccccccccccccccccccccccc$	¹³ CH ₃ OH						
$\begin{array}{cccccccccccccccccccccccccccccccccccc$	156.299374	5 ₀₅ -5 ₋₁₅	0.697	47.1	0.19 ± 0.08	65	3.0 ± 0.5
$\begin{array}{cccccccccccccccccccccccccccccccccccc$	160.507694	2_{12} -3_{03}	0.300	21.3	0.08 ± 0.02	29	2.4 ± 0.6
$\begin{array}{cccccccccccccccccccccccccccccccccccc$	330.194042	7_{-17} – 6_{-16}	5.55	69.0	0.51 ± 0.16	120	3.8 ± 0.6
$\begin{array}{cccccccccccccccccccccccccccccccccccc$	330.252798	7_{07} – 6_{06}	5.66	63.4	0.43 ± 0.15	100	4.0 ± 1.2
$\begin{array}{cccccccccccccccccccccccccccccccccccc$	330.265233	7_{-61} – 6_{-60}	1.50	253.4	0.15 ± 0.10	80	1.7 ± 1.0
$\begin{array}{cccccccccccccccccccccccccccccccccccc$	330.277270	7_{61} – 6_{60}	1.50	258.1	0.12 ± 0.08	60	2.0 ± 0.7
$\begin{array}{cccccccccccccccccccccccccccccccccccc$	330.277270	7_{62} – 6_{61}	1.50	258.1	0.12 ± 0.08	60	2.0 ± 0.7
$\begin{array}{cccccccccccccccccccccccccccccccccccc$	330.319110	7_{52} – 6_{51}	2.78	202.0	0.45 ± 0.21	90	4.8 ± 0.9
$\begin{array}{cccccccccccccccccccccccccccccccccccc$	330.319110	7_{53} – 6_{52}	2.78	202.0	0.45 ± 0.21	90	4.8 ± 0.9
$\begin{array}{cccccccccccccccccccccccccccccccccccc$	330.342534	7_{44} – 6_{43}	3.81	144.2	0.07 ± 0.05	50	1.3 ± 6.7
$\begin{array}{cccccccccccccccccccccccccccccccccccc$	330.342534		3.81	144.2	0.07 ± 0.05	50	1.3 ± 6.7
330.442421 7_{16} -6 ₁₅ 5.69 84.49 0.42 ± 0.12 140 2.8 ± 0.9 330.535822 7_{25} -6 ₂₄ 5.14 85.80 0.25 ± 0.11 40 5.6 \pm 1.2	330.408395	7_{34} – 6_{33}	4.61	111.4	0.91 ± 0.19	200	4.2 ± 0.7
330.535822 7_{25} - 6_{24} 5.14 85.80 0.25 ± 0.11 40 5.6 ± 1.2	330.442421			84.49	0.42 ± 0.12	140	2.8 ± 0.9
	330.535822			85.80	0.25 ± 0.11	40	5.6 ± 1.2
	330.535890	7 ₋₂₆ -6 ₋₂₅	5.20	89.45	0.25 ± 0.11	40	5.6 ± 1.2

¹ The fluxes were derived using Gaussian fits, and the uncertainty given is $\sqrt{\sigma_{\text{stat}}^2 + \sigma_{\text{cal}}^2}$ where σ_{stat} is the statistical error and σ_{cal} the calibration uncertainty (15%). ² The noise rms is 8 mK for the CD₃OH data and 37 mK for the ¹³CH₃OH data. ³ A star following the frequency indicates that the line is close to a CH₂DCN line and was fitted by a two-component Gaussian fit (see text).

2. Observations and results

Using the IRAM 30-meter telescope (Pico Veleta, Spain), we detected the 12 CD₃OH lines reported in Table 1. The telescope was pointed at the coordinates $\alpha(2000) = 16^{\text{h}}32^{\text{m}}22.6^{\text{s}}$ and $\delta(2000) = -24^{\circ}28'33.0''$. The observations were performed in April 2003. Two receivers were used simultaneously at 2 mm, to observe two bands around 156 and 160 GHz, with typical system temperatures of about 230 and 250 K respectively. These receivers were connected to the VESPA autocorrelator divided in six units. The telescope beam width is approximately 15" at 160 GHz. All observations were performed using the wobbler switching mode with an OFF position 4' from the source. The pointing accuracy was monitored regularly on strong continuum sources, and was found to be better than 3". All spectra were obtained with an integration time of 750 min. The rms noise is equal to 8 mK $(T_{\rm mb})$ for a spectral resolution of 0.3 km s^{-1} .

Observed spectra are shown in Fig. 1. The measured intensities, linewidths and main-beam temperatures are reported in Table 1. The frequencies of all detected lines have previously been measured in the laboratory with an accuracy of 25 kHz (Walsh et al. 1998), while the transition strengths and energy levels were estimated from the published spectroscopic constants (Predoi-Cross et al. 1998) using the methanol program at Ohio State.

Some of the CD_3OH lines (indicated by a star in Table 1) are close to CH_2DCN lines. In that case, the intensity was derived by using a two-component Gaussian fit, so the quoted fluxes have a further uncertainty due to the relative line contribution.

Two ¹³CH₃OH lines at 156 GHz were observed simultaneously to the CD₃OH lines. In addition, we analysed 330 GHz ¹³CH₃OH observations obtained using the JCMT in January 2000, with an rms noise of 37 mK. The beam size of the JCMT is 15" at the considered frequencies, i.e. equivalent

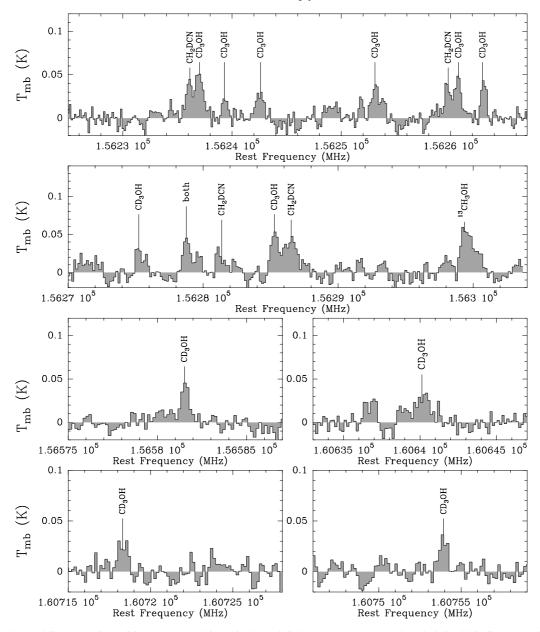


Fig. 1. CD_3OH detected lines. The intensities are reported in main-beam brightness temperature. The label "both" indicates the blending of one CD_3OH and one CH_2DCN lines. This latter CD_3OH line has not been considered in the population diagram analysis.

to the beam size of the 30-meter at 160 GHz. Detailed information concerning the ¹³CH₃OH spectra is presented in Table 1.

3. Derivation of the column densities

We derived the abundance of CD₃OH using the method of rotational diagrams. The A and E species are considered to be linked by ion-molecule reactions that transfer molecules from one species to the other. We then computed one single rotational diagram for the two species, presented in Fig. 2a. We averaged the level column densities on a 10" beam, as in Parise et al. (2002), following the suggestion by van Dishoeck et al. (1995) of enhanced methanol emission in the central 10" region of IRAS 16293. A more recent study of the spatial distribution of CH₃OH was performed by Schoier et al. (2002), and showed evidence for an abundance

jump of methanol of two orders of magnitude in the inner part of the envelope (≤150 AU). However, in the following we consider averaged abundances on a 10" beam for consistency with the Parise et al. (2002) study.

The ground E state is estimated to lie about 4.6 K above the ground A state. An A state has a relative spin-torsional weight of 11 whereas the relative spin-torsional weight of an E state is 16. The partition function was computed from the asymmetric-top approximation:

$$Z(T) = 11 \times Z_{A}(T) + 16 \times \exp(-4.6/T) \times Z_{E}(T)$$

where $Z_A(T) = Z_E(T) = \sqrt{\frac{\pi T^3}{ABC}}$, with A = 3.3957 K, B = 0.9529 K and C = 0.9247 K, as determined by Walsh et al. (1998).

By fitting a straight line to the data in the rotational diagram, we derive a rotational temperature of 85 ± 28 K,

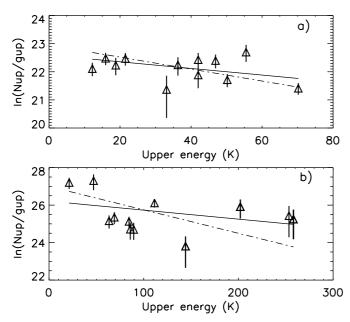


Fig. 2. Rotational diagram for: **a)** CD₃OH (solid line $T_{\rm rot} = 85$ K, dashed line: $T_{\rm rot} = 47$ K, see text), **b)** 13 CH₃OH (solid line: $T_{\rm rot} = 208$ K, dashed line: $T_{\rm rot} = 80$ K, see text). Column densities are averaged on a 10'' beam.

Table 2. Derived column densities and fractionation ratios relative to CH₃OH for deuterated methanols in IRAS 16293.

Molecule	$T_{\rm rot}({ m K})$	$N (\mathrm{cm}^{-2})$	fractionation
CD_3OH	85 ± 28	$(1.4 \pm 0.9) \times 10^{14}$	$1.4\pm1.4\%$
	47 ± 7^a	$(7.8 \pm 2.3) \times 10^{13}$	$0.8\pm0.6\%$
$\mathrm{CHD}_2\mathrm{OH}^b$	47 ± 7	$(6.0 \pm 2.2) \times 10^{14}$	$6 \pm 5\%$
$\mathrm{CH}_2\mathrm{DOH}^b$	48 ± 3	$(3.0 \pm 0.6) \times 10^{15}$	$30\pm20\%$
CH_3OD^b	20 ± 4	$(1.5 \pm 0.7) \times 10^{14}$	$2 \pm 1\%$

^a Fixed temperature, see text. ^b Observed in Parise et al. (2002).

consistent with the rotational temperature of CH₃OH (van Dishoeck et al. 1995). The CD₃OH column density is $(1.4 \pm 0.9) \times 10^{14}$ cm⁻². We also derived the CD₃OH column density by fixing the rotational temperature to the one inferred from the CH₂DOH and CHD₂OH molecules ($T_{\rm rot} = 47 \pm 7$ K, Parise et al. 2002). The CD₃OH column density is then $(7.8 \pm 2.3) \times 10^{13}$ cm⁻². Table 2 lists the column densities for all deuterated methanols observed in IRAS 16293.

The column density of $^{13}\text{CH}_3\text{OH}$ was derived using the same method, with the molecular parameters taken from the Cologne Database for Molecular Spectroscopy (Muller et al. 2001). The rotational diagram is presented in Fig. 2b. The inferred rotational temperature is 208 ± 70 K and the column density averaged over a 10'' beam is $(2.6\pm1.8)\times10^{14}$ cm $^{-2}$. We also computed the column density for fixed rotational temperatures of 50 K and 80 K. The inferred value is $(1.4\pm0.6)\times10^{14}$ cm $^{-2}$, independent of the temperature in this range. Using the $^{12}\text{C}/^{13}\text{C}$ ratio of 70 derived by Boogert et al. (2002), we derive a column density of $(9.8\pm4.2)\times10^{15}$ cm $^{-2}$ for CH₃OH. This value is nearly 3 times higher than the column density used by Parise et al. (2002), inferred from CH₃OH

observations from van Dishoeck et al. (1995). The fractionation ratios, relative to this new estimate of the CH₃OH column density, are reported in Table 2 for all deuterated isotopomers of methanol.

4. Discussion and conclusions

The main result of this Paper is the first detection of triply-deuterated methanol in space, with 12 detected transitions. This discovery follows the detection of doubly-deuterated as well as singly-deuterated isotopomers towards the same object (Parise et al. 2002). Observations of multiple isotopomers of methanol represent a powerful constraining tool for chemical processes that lead to such a high deuteration.

It is interesting to compare these observations to the predictions of the simple grain chemistry scheme of Rodgers & Charnley (2002). If the D atoms are randomly distributed in the methanol isotopomers (i.e. this scheme does not consider any activation barrier for the reactions but rather assumes that all reactions are equiprobable), the fractionation ratios R of each isotopomer relative to CH₃OH should scale as follows: $R(CH_3OD) = \alpha$, $R(CH_2DOH) = 3\alpha$, $R(CHD_2OH) =$ $3\alpha^2$ and $R(CD_3OH) = \alpha^3$, where α is the accreting atomic D over H ratio. The three independent observations of CH₂DOH, CHD₂OH and CD₃OH are consistent within the error bars with a value of 0.1–0.2 for the D over H accretion rate. Accounting for the different mass of the atoms, this ratio corresponds to an abundance ratio in the gas-phase of D/H = $\sqrt{2} \times (0.1-0.2)$ = 0.15-0.3. However, this simple scheme fails to explain the observed low abundance of CH₃OD.

More accurate grain chemical models accounting for different activation barriers for the reactions have been developed in the last few years. We compare in the following our observations with the model developed by Stantcheva & Herbst (2003). This model is based on the direct solution of the master equation and therefore gives essentially the same predictions as the Monte Carlo models described by Caselli et al. (2002) or Charnley et al. (1997). Figure 3 shows predictions for fractionation ratios of deuterated isotopomers of methanol relative to CH₃OH versus the atomic D/H ratio in the accreting gas (Stantcheva & Herbst 2003) when the various isotopomers are formed by active grain chemistry. In the limit of low temperature (10 K), this model essentially gives the ratios corresponding to a random distribution of deuterium atoms. Observed fractionation ratios with their error bars have been overlaid on each curve, allowing the derivation of the required atomic D/H ratio in the gas-phase. The CD₃OH, CHD₂OH and CH₂DOH observations are consistent with a formation on grain surfaces with an atomic D/H abundance ratio of 0.1-0.2. Such a high atomic fractionation ratio in the gas phase is predicted by the recent gas-phase model of Roberts et al. (2003), which involves not only H₂D⁺ but also D₂H⁺ and D₃⁺ as precursors for deuterium fractionation, when the density of gas is very high and heavy species such as CO are strongly depleted.

As can be seen in Fig. 3, CH_3OD appears to be underdeuterated when compared with the grain chemical predictions. It is possible that the CH_3OD fractionation may be affected in the warm gas; e.g., this isotopomer may be preferentially converted into CH_3OH when released in the gas-phase by

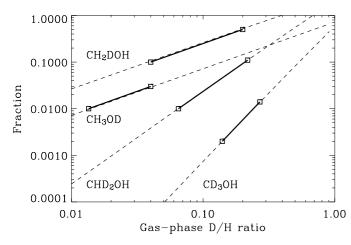


Fig. 3. The deuterium fractionation ratio for the various deuterated isotopomers of methanol is plotted against the abundance ratio of deuterium to hydrogen atoms in the gas phase. Dashed lines: model results of Stantcheva et al. (2003). Thick lines: observations of IRAS 16293.

protonation reactions followed by dissociative recombination with an electron (Charnley et al. 1997; Parise et al. 2002):

$$CH_3OD + H_3^+ \rightarrow CH_3ODH^+ + H_2$$

 $CH_3OHD^+ + e^- \rightarrow CH_3OH + D.$

The corresponding reactions with H_2D^+ , HD_2^+ and D_3^+ are of little importance in view of their low abundance in the warm gas of the hot core. This hypothesis, which assumes that protonation reactions attack the oxygen end of the methanol only (Osamura et al. in prep.), could be tested by observing the CH_2DOD isotopomer. This observation may be difficult due to the expected low intensity of the lines.

Acknowledgements. E. Herbst acknowledges the support of the National Science Foundation (US) for his research program in astrochemistry.

References

Bacmann, A., Lefloch, B., Ceccarelli, C., et al. 2002, A&A, 389, L6 Bacmann, A., Lefloch, B., Ceccarelli, C., et al. 2003, ApJ, 585, L55

Boogert, A. C. C., Blake, G. A., & Tielens, A. G. G. M. 2002, ApJ, 577, 271

Caselli, P., Stantcheva, T., Shalabiea, O., et al. 2002, Planet. Space Sci., 50, 1257

Caselli, P., van der Tak, F. F. S., Ceccarelli, C., & Bacmann, A. 2003, A&A, 403, L37

Cazaux, S., Tielens, A. G. G. M., Ceccarelli, C., et al. 2003, ApJL, in press

Ceccarelli, C., Vastel, C., Tielens, A. G. G. M., et al. 2002, A&A, 381, L17

Ceccarelli, C., Loinard, L., Castets, A., et al. 2001, A&A, 372, 998Ceccarelli, C., Castets, A., Loinard, L., Caux, E., & Tielens, A. G. G. M. 1998, A&A, 338, L43

Charnley, S. B., Tielens, A. G. G. M., & Rodgers, S. D. 1997, ApJ, 482, L203

Linsky, J. L. 1998, Space Sci. Rev., 84, 285

Lis, D. C., Roueff, E., Gerin, M., et al. 2002, ApJ, 571, L55

Loinard, L., Castets, A., Ceccarelli, C., Caux, E., & Tielens, A. G. G. M. 2001, ApJ, 552, L163

Loinard, L., Castets, A., Ceccarelli, C., et al. 2000, A&A, 359, 1169 Maret, S., et al. in preparation

Muller, H. S. P., Thorwirth, S., Roth, D. A., & Winnewisser, G. 2001, A&A, 370, L49

Parise, B., Ceccarelli, C., Tielens, A. G. G. M., et al. 2002, A&A, 393, L49

Phillips, T., & Vastel, C. 2003, in Chemistry as a Diagnostic of Star Formation, ed. C. L. Curry & M. Fish, in press [astro-ph/0211610]

Predoi-Cross, A., Xu. L.-H., Walsh, M. S., et al.. 1998, J. Mol. Spec., 188, 94

Roberts, H., Herbst, E., & Millar, T. J. 2003, ApJ, 591, 41

Rodgers, S. D., & Charnley, S. B. 2002, Planet. Space Sci., 50, 1125

Roueff, E., Tiné, S., Coudert, L. H., et al. 2000, A&A, 354, L63

Schoier, F. L., Jorgensen, J. K., van Dishoeck, E. F., & Blake, G. A. 2002, A&A, 390, 1001

Stantcheva, T., & Herbst, E. 2003, MNRAS, 340, 983

van der Tak, F. F. S., Schilke, P., Müller, H. S. P., et al. 2002, A&A, 388, L53

van Dishoeck, E. F., Blake, G. A., Jansen, D. J., & Groesbeck, T. D. 1995, ApJ, 447, 760

Vastel, C., Phillips, T. G., Ceccarelli, C., & Pearson, J. 2003, ApJ, 593, L97

Walsh, M. S., Xu, L.-H., & Lees, R. M. 1998, J. Mol. Spectrosc., 188, 85